

Observations from the Analyses of Magnetic Field and AC Loss Distributions in the NHMFL 32 T All-Superconducting Magnet HTS Insert

Andrew V. Gavrilin, Jun Lu, Hongyu Bai, David K. Hilton, W. Denis Markiewicz, and Hubertus W. Weijers

Abstract—A 17 T high-temperature superconducting two-coil magnet (insert) to be operated in a 15 T low-temperature superconducting multisection magnet (outsert) is the most demanding part of the National High Magnetic Field Laboratory all-superconducting 32 T magnet system. The HTS coils are of the pancake type and to be wound with REBCO coated conductors/tapes manufactured by SuperPower, Inc. The distribution of AC losses in the HTS windings during the magnet charging/discharging process are computed and analyzed with due regard for the AC loss density dependence on the magnetic field and the field angle. The calculations are based on the measured magnetization of a representative sample against magnetic field and field angle. The results enable determination of heat load on the magnet and its cryogenic system. Since the magnet is of the pool-cooled type, a related helium vapor bubble problem can develop owing to the high field and field gradients, and the diamagnetic susceptibility of helium.

Index Terms—Field angle, helium diamagnetic susceptibility, high magnetic field, hysteresis loss, REBCO coil, superconducting magnet.

I. INTRODUCTION

THE NHMFL 32 T all-superconducting magnet [1] being developed presently will be made up of an HTS insert, which is presumed to give 17 T of field, and a 15 T LTS background field outsert (outer magnet) (Fig. 1). It is planned to use two power supplies: one is for the insert and the other—for the outsert. It enables one to ramp the insert and outsert up to the field and down independently of one another, if required, or concurrently as a normal operation scenario. The updated design parameters of the HTS insert are given in Table I. Test and prototype coils (Fig. 1) were built in the course of the insert development with a view to testing the validity and optimality of the design concepts.

The HTS insert is envisioned to consist of two coils (a shorter inner coil, “Coil 1” and a longer outer coil, “Coil 2”) pancake-wound with 4.1 mm wide REBCO coated bare conductor/tape supplied by SuperPower, Inc. (SP) [1], [2].

Manuscript received October 5, 2012; accepted January 24, 2013. Date of publication January 30, 2013; date of current version March 13, 2013. This work was supported in part by the State of Florida and by the U.S. National Science Foundation under Grants DMR-0654118 and DMR-0923070.

The authors are with the National High Magnetic Field Laboratory, Florida State University, Tallahassee, FL 32310 USA (e-mail: gavrilin@magnet.fsu.edu; junlu@magnet.fsu.edu; bai@magnet.fsu.edu; dkhilton@magnet.fsu.edu; markwcz@magnet.fsu.edu; weijers@magnet.fsu.edu).

Color versions of one or more of the figures in this paper are available online at <http://ieeexplore.ieee.org>.

Digital Object Identifier 10.1109/TASC.2013.2244154

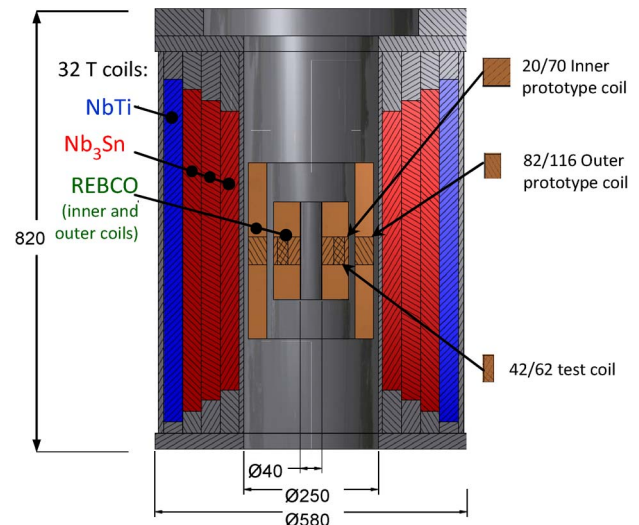


Fig. 1. Cross-section of the 32 T magnet with the LTS outsert (preliminary design concept by OI) and the HTS insert REBCO coils. REBCO test and prototype coils built in the course of HTS insert development are shown, too: “20/70”, “82/116”, and “42/62” denote the inner and outer radii of the prototype and test coils, respectively. All dimensions are in mm.

TABLE I
PARAMETERS OF HTS INSERT COILS AND REBCO CONDUCTOR USED

| HTS insert | Coil 1 | Coil 2 |
|--|--------|--------|
| Inner radius (mm) | 20 | 82 |
| Outer radius (mm) | 70 | 116 |
| Coil length (mm) | 178 | 320.4 |
| Number of pancakes/disks | 40 | 72 |
| Turns per disk | 244 | 148 |
| Conductor length per disk (m) | 69 | 92 |
| Average current density (A/mm ²) | 197 | 176 |
| REBCO conductor and inter-turn insulation | | |
| Conductor width (mm) | ~ 4.1 | |
| Conductor thickness (μm) | 155 | |
| SS tape thickness (μm) | 25 | |
| Thickness of sol-gel layer per side (μm) | ~ 3 | |
| Total thickness of coated SS tape (μm) | ~ 32 | |

For the inter-turn insulation a sol-gel alumina insulated co-wound stainless steel tape of the same width is to be applied [1], [2]. The REBCO coils assembled from a rather large number of pancakes (Table I) are supposed to be non-impregnated (with epoxy resin) to avoid the de-lamination force on the tape [1], [2]. The inner coil (Coil 1) is presumed to have a 2 mm split.

The LTS outsert will be a combination of Nb₃Sn and NbTi coils. There are two key requirements to the outsert: (a) it should be capable of absorbing the stored energy of the insert during quench and survive, being appropriately quench-protected, and (b) to generate a rather uniform background field to reduce the field angle (see below) in the insert windings so as to minimize the AC losses in them while ramping up and/or down.

The AC loss calculation results presented in this paper are obtained using one of the latest NHMFL configurations of the outsert, which was just employed to design the insert. However, the production outsert will be developed and built by Oxford Instruments Nanotechnology Tools, Ltd. (OI) working presently on the design. We hope that the OI's outsert will furnish the desired field magnitude with slightly smaller average field angle in the insert area than we obtained, which correspondingly will result in somewhat lower AC losses. Thus, the calculation results given below may turn out to be slightly conservative.

II. AC LOSS DEPENDENCE ON MAGNETIC FIELD AND MAGNETIC FIELD ANGLE

It is anticipated that AC losses in the insert REBCO coils, when ramping the magnet up to the field and/or down, will be significant. The hysteresis loss in the tape was quantified by means of magnetization measurements [3]. The measurements were performed by a vibrating sample magnetometer (VSM) in the Quantum Design Physical Property Measurement System (PPMS) at 4.22 K in a $+/-9$ T field cycle. A 1 mm by 1 mm sample was cut from the REBCO tape. The sample was glued to a holder which is mounted to the VSM rod at different angles. The measured hysteresis loss density (in J/m) for a $0 - B$ (or $B - 0$) ramp ("one quadrant ramp") against the field magnitude B and the field angle θ_1 is fitted with the following function, $Q_{hyst}(B, \theta_1)$ (in the absence of transport current and at the fixed temperature) [3]:

$$Q_{hyst}(B, \theta_1) = \frac{K}{4} w \sin \theta_1 \int_0^B I_C(B', \theta) dB', \quad (1)$$

$$I_C(B, \theta) = b_0 (B + \beta_0)^{-\alpha_0} + \frac{b_1}{(B + \beta_1)^{\alpha_1} \sqrt{\omega_1^2(B) \cos^2(\theta - \varphi_1) + \sin^2(\theta - \varphi_1)}}, \quad (2)$$

$$\omega_1(B) = c_1 \left(B + c_1^{-5/3} \right)^{3/5}$$

where $I_C(B, \theta)$ is the critical current dependence on B and θ at 4.2 K [4], [5]; w is the superconducting area width (taken equal to 4 mm) in the tape, $\theta_1 = \pi/2 - \theta$ is the angle between

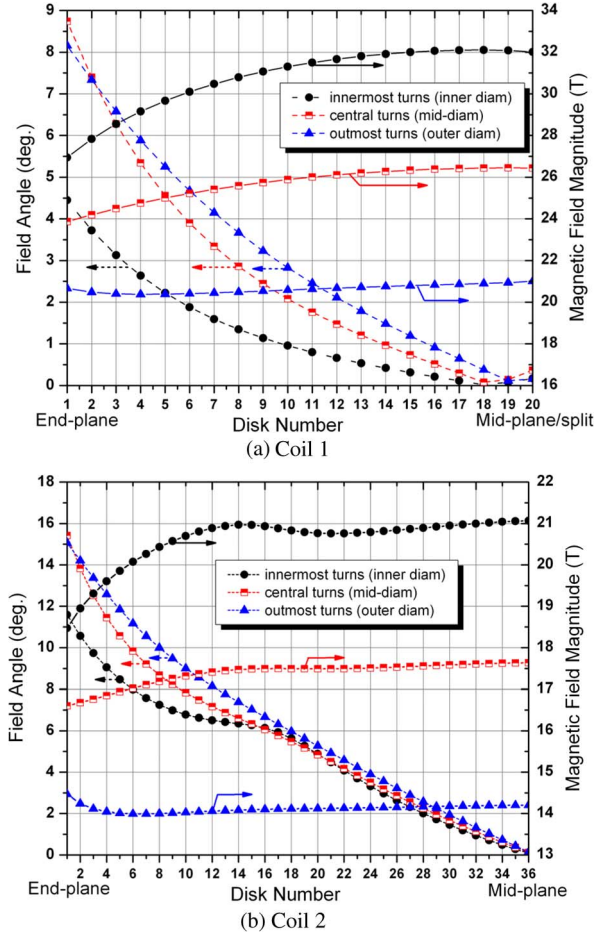


Fig. 2. Axial distributions of the magnetic field and the field angle on the outer diameter, mid-diameter, and inner diameter of Coil 1 (a) and Coil 2 (b) of the insert at the full current. The background field from the outsert is included (normal operation scenario: the insert and the outsert are energized simultaneously, Case A).

the field vector and the ab -plane of the superconductor (the right angle, $\theta_1 = \pi/2$, corresponds to the field vector normal to the tape surface). The fit parameter K is found to be taken equal to 0.88 in order to reach a satisfactory agreement between the measurements and the calculation results [3]. The K -value is below 1 due to the difference between magnetization and transport measurements. The values of fit parameters b_0 , b_1 , α_0 , α_1 , β_0 , β_1 , c_1 , and φ_1 used in the calculations are for the SP-26 tape [4], [5]. Also, no magnetization loss dependence on the ramp rate was really observed so far: i.e., practically no any significant AC losses in the REBCO coils are expected but the hysteresis one, and yet it is bound to increase somewhat, if the transport current is taken into account [3].

III. HYSTERESIS LOSS IN THE INSERT REBCO COILS WHEN RAMPING UP OR DOWN

Formulae (1) and (2) enable us to calculate precisely the hysteresis loss in the HTS coils during the process of charging or discharging, or both, provided detailed spatial distributions of the magnetic field and the field angle, which are rather non-uniform, are computed. The total hysteresis loss in Coil 1

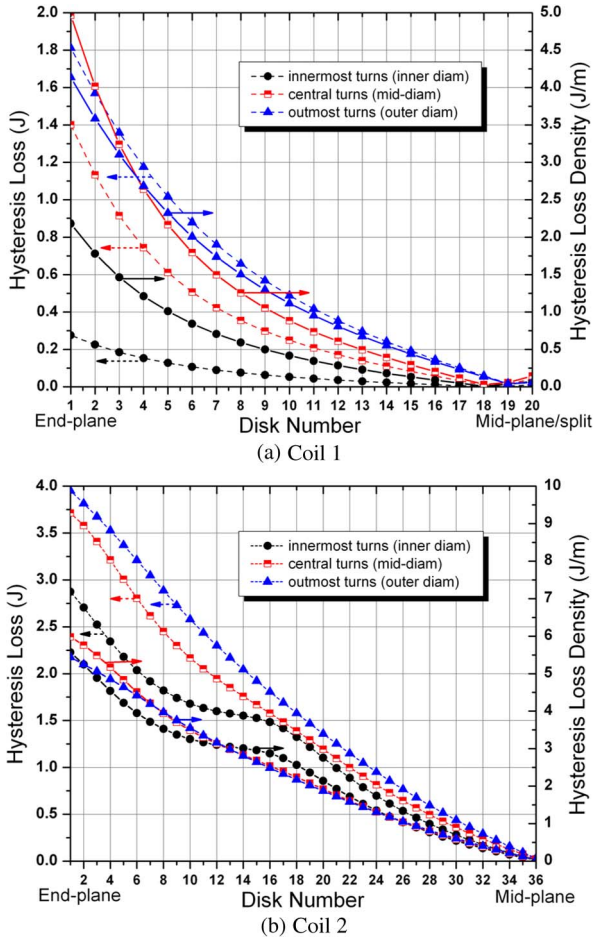


Fig. 3. Axial distributions of the AC loss and the AC loss density on the outer diameter, mid-diameter, and inner diameter of Coil 1 (a) and Coil 2 (b) of the insert as a result of ramping the magnet up to the full field. Normal operation scenario: the insert and the outsert are energized simultaneously, Case A.

and Coil 2 are calculated through integration over the volume of Coil 1 and Coil 2, to be specific, by summing over all the turns:

$$E_{hyst}^{1,2} = 2\pi \sum_{n=1}^{N^{1,2}} R_n Q_{hyst} \left(B^{(n)}, \theta_1^{(n)} \right), \theta_1^{(n)} = \text{atan} \left| \frac{B_R^{(n)}}{B_Z^{(n)}} \right| \quad (3)$$

where $N^{1,2}$ is the total number of turns in Coils 1 & 2, respectively; $\theta_1^{(n)}$ is the field angle at a turn with the ordinal number n , $B_R^{(n)}$ and $B_Z^{(n)}$ are the radial and axial components of the field with magnitude $B^{(n)}$ at the turn, R_n is the turn radius.

As can be inferred from Fig. 2, there are rather non-uniform distributions of the field and hence those of the field angle, which result in significant non-uniformity of the hysteresis loss distributions in the HTS coils (Fig. 3), especially in Coil 2.

It is worthy of notice that the angular dependence of the loss is important, and by reducing the average field angle in the coils one can bring the total hysteresis loss noticeably down. Indeed, in the case of normal operation, when both the insert and the outsert are energized simultaneously (Case A, Table II), the field in the HTS coils is the highest, however, the field distributions within the coils are much more uniform (smaller field angles) than in the case when the outsert is not

TABLE II
AC LOSS IN REBCO COILS DUE TO RAMPING UP TO FULL FIELD @ 4.2 K

| With background field (Case A) | Coil 1 | Coil 2 |
|------------------------------------|--------|--------|
| Total AC loss (kJ), E_{hyst} | 3.48 | 15.31 |
| Maximum field in coil (T) | 32.10 | 21.07 |
| Average field in coil (T) | 25.65 | 17.35 |
| Average radial field in coil (T) | 1.09 | 1.68 |
| Maximum field angle in coil (deg.) | 9.27 | 15.87 |
| Average field angle in coil (deg.) | 2.57 | 5.66 |
| Average density of AC loss (J/m) | 1.26 | 2.31 |
| Without background field (Case B) | Coil 1 | Coil 2 |
| Total AC loss (kJ), E_{hyst} | 4.38 | 11.90 |
| Maximum field in coil (T) | 17.14 | 6.48 |
| Average field in coil (T) | 10.82 | 3.06 |
| Average radial field in coil (T) | 0.99 | 1.26 |
| Maximum field angle in coil (deg.) | 25.11 | 89.80 |
| Average field angle in coil (deg.) | 6.10 | 33.12 |
| Average density of AC loss (J/m) | 1.59 | 1.80 |

energized, providing no background field (Case B, Table II). As a result, the hysteresis loss in the insert in Case A (when the field is maximal) is only slightly higher than in Case B (when the field strength is much smaller): 18.8 kJ against 16.3 kJ (that costs 6.1 liters and 5.3 liters of liquid helium (LHe), respectively). Thus, by improving the outsert design so as to furnish the most uniform field that is possible in the insert coils, one can reduce the hysteresis losses. At the same time, one important point to remember is that the hysteresis loss density dependence on temperature is disregarded in the simplified model we used. Clearly, the temperature rises, as heat caused by the AC losses is evolved in the HTS coils, not to mention that the coil thermal conduction [2] may have a pronounced effect on the temperature profile and hence on the AC loss power density distribution with space and time. These factors neglected yet are apt to halve roughly the total hysteresis loss in the REBCO coils [3].

As Fig. 3 suggest, the highest AC losses occur near the end-planes of the coils. Thus, presumably, by effectively cooling the coils' edges, one can likely prevent a significant rise in the winding temperature by virtue of a rather high axial thermal conduction of the coils [2]. From this perspective, the next task will be to calculate the temperature changes resulting from the AC losses in the coils that invites a comprehensive transient non-linear thermal analysis including the thermal conduction and heat transfer to LHe [3] as well at different values of the current ramp rate, aiming to figure out to what extent the AC losses at this level are really an issue (particularly, could they quench the insert), but in one way or another the AC loss generation will definitely contribute to another problem we will take a look at in the next section.

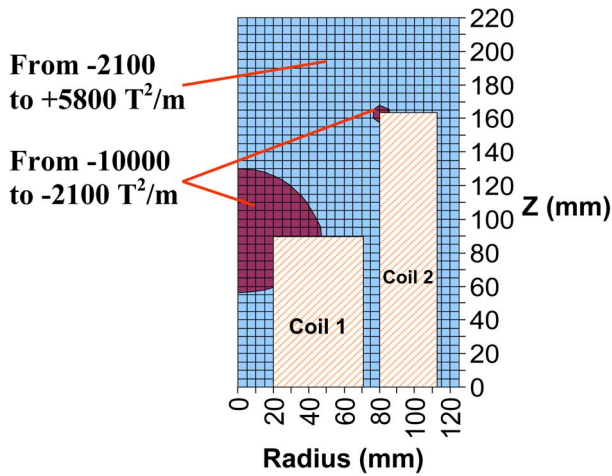


Fig. 4. Regions of $B_z \partial B_z / \partial z < -2100 \text{ T}^2/\text{m}$ in the 32 T magnet. The upper half of each REBCO coil is shown.

IV. HELIUM VAPOR BUBBLE ISSUE

The AC losses in the REBCO coils, Joule heat generated in the numerous internal joints [1], [2], and heat input from the current leads as well are absorbed by LHe, utilizing its latent heat of vaporization. This gives birth to helium vapor bubbles which are supposed to rise to the LHe bath surface. However, this mechanism of the heat removal can be hampered due to the diamagnetic susceptibility of helium [6]. There are two regions at the magnet bore entrance where the value of $B_z \partial B_z / \partial z$ is expected to be less than $-2100 \text{ T}^2/\text{m}$ (Fig. 4), at the rated currents in the insert and outsert. In these regions the bubbles can be trapped [6], forming rather large super-bubbles (“bubble areas,” Fig. 4) which will grow in size in their quest to fill the entire regions where $B_z \partial B_z / \partial z < -2100 \text{ T}^2/\text{m}$. Owing to a rather poor cooling capability of the vapor compared to that of LHe, the coils may turn out to be too poorly cooled in the bubble areas to maintain the temperature at a sufficiently low level. Thus, we ought to enhance the heat removal efficiency in the bubble areas.

Presumably, there exist two ways to do it: (a) by removing the bubbles away, and (b) by conducting the heat away from the bubble areas using a material with a very high thermal conductivity. The first way would require a cryogenic pump or a pressurized cryostat, and other equipment as well, to be integrated with the magnet system. This expedient would also bring about a noticeable rise in heat load to the cryostat, i.e., markedly higher LHe consumption rates. The second way

seems to be a better choice, because it is a relatively simple one and additional losses associated with this approach are practically negligible. To be specific, the suggestion is to use thin copper strips going from the LHe areas to the bubble areas that is tried in our prototype coils.

V. CONCLUSION

Hysteresis losses in the REBCO coils of the NHMFL 32 T all-superconducting magnet, which occur while charging/discharging the magnet, were calculated and discussed. The losses are significant, and their impact on the REBCO coils performance should be scrutinized with the use of detailed transient thermal analysis. A related issue of accumulation of helium vapor bubbles on the REBCO coil surface is recognized also: provisions will be made to prevent trapping the bubbles so as to enhance efficiency of the heat removal from the coils.

ACKNOWLEDGMENT

The authors thank M. D. Bird and D. C. Larbalestier for encouraging the work, support, and valuable technical discussions.

REFERENCES

- [1] W. D. Markiewicz, D. C. Larbalestier, H. W. Weijers, A. J. Voran, K. W. Pickard, W. R. Sheppard, J. J. Jaroszynski, A. Xu, R. P. Walsh, J. Lu, A. V. Gavrilin, and P. D. Noyes, “Design of a superconducting 32 T magnet with REBCO high field coils,” *IEEE Trans. Appl. Supercond.*, vol. 22, no. 3, p. 4300704, Jun. 2012.
- [2] H. Bai, W. D. Markiewicz, J. Lu, and H. W. Weijers, “Thermal conductivity test of YBCO coated conductor tape stacks interleaved with insulated stainless steel tapes,” presented at the Appl. Supercond. Conf., Portland, OR, USA, 2012, Paper 2LPQ-01.
- [3] J. Lu, D. V. Abramov, A. A. Polyanskii, A. V. Gavrilin, D. K. Hilton, W. D. Markiewicz, and H. W. Weijers, “Field angular dependence of hysteresis loss of coated conductor for high field magnets,” presented at the Appl. Supercond. Conf., Portland, OR, USA, 2012, Paper 2MPA-05.
- [4] D. K. Hilton, U. P. Trociewitz, J. J. Jaroszynski, A. Xu, H. W. Weijers, and D. C. Larbalestier, “Practical fit functions for transport critical current vs. field and angle data from REBCO tape conductors at fixed low temperatures in high magnetic fields,” presented at the 22nd Int. Conf. Magnet Technol. (MT-22), IIO2-1, Marseille, France, Sep. 12, 2011.
- [5] D. K. Hilton, U. P. Trociewitz, J. J. Jaroszynski, A. Xu, H. W. Weijers, and D. C. Larbalestier, “Practical fit functions for transport critical current versus field and angle data from (RE)BCO coated conductors at fixed low temperatures in high magnetic fields,” *Supercond. Sci. Technol.*, submitted for publication.
- [6] E. J. McNiff, B. L. Brandt, S. Foner, L. G. Rubin, and R. J. Wegel, “Temperature anomalies observed in liquid ^4He columns in magnetic fields with field-field-gradient products $> 21 \text{ T}^2/\text{cm}$,” *Rev. Sci. Instrum.*, vol. 59, no. 11, p. 2474–2476, Nov. 1988.